Seasonal Shifts in the North American Monsoon

KATRINA GRANTZ
Department of Civil, Environmental, and Architectural Engineering, and Center for Advanced Decision Support for Water and Environmental Systems, University of Colorado, Boulder, Colorado

BALAJI RAJAGOPALAN
Department of Civil, Environmental, and Architectural Engineering, and CIRES, University of Colorado, Boulder, Colorado

MARTYN CLARK
CIRES, University of Colorado, Boulder, Colorado

EDITH ZAGONA
Department of Civil, Environmental, and Architectural Engineering, and Center for Advanced Decision Support for Water and Environmental Systems, University of Colorado, Boulder, Colorado

(Manuscript received 6 January 2006, in final form 7 July 2006)

ABSTRACT

Analysis is performed on the spatiotemporal attributes of North American monsoon system (NAMS) rainfall in the southwestern United States. Trends in the timing and amount of monsoon rainfall for the period 1948–2004 are examined. The timing of the monsoon cycle is tracked by identifying the Julian day when the 10th, 25th, 50th, 75th, and 90th percentiles of the seasonal rainfall total have accumulated. Trends are assessed using the robust Spearman rank correlation analysis and the Kendall–Theil slope estimator. Principal component analysis is used to extract the dominant spatial patterns and these are correlated with antecedent land–ocean–atmosphere variables. Results show a significant delay in the beginning, peak, and closing stages of the monsoon in recent decades. The results also show a decrease in rainfall during July and a corresponding increase in rainfall during August and September. Relating these attributes of the summer rainfall to antecedent winter–spring land and ocean conditions leads to the proposal of the following hypothesis: warmer tropical Pacific sea surface temperatures (SSTs) and cooler northern Pacific SSTs in the antecedent winter–spring leads to wetter than normal conditions over the desert Southwest (and drier than normal conditions over the Pacific Northwest). This enhanced antecedent wetness delays the seasonal heating of the North American continent that is necessary to establish the monsoonal land–ocean temperature gradient. The delay in seasonal warming in turn delays the monsoon initiation, thus reducing rainfall during the typical early monsoon period (July) and increasing rainfall during the later months of the monsoon season (August and September). While the rainfall during the early monsoon appears to be most modulated by antecedent winter–spring Pacific SST patterns, the rainfall in the later part of the monsoon seems to be driven largely by the near-term SST conditions surrounding the monsoon region along the coast of California and the Gulf of California. The role of antecedent land and ocean conditions in modulating the following summer monsoon appears to be quite significant. This enhances the prospects for long-lead forecasts of monsoon rainfall over the southwestern United States, which could have significant implications for water resources planning and management in this water-scarce region.

1. Introduction and background

The North American monsoon system (NAMS) is the large-scale atmospheric circulation system that drives the dramatic increase in rainfall experienced in the desert southwest United States and northwestern Mexico during the summer months of July, August, and September. These summer thunderstorms typically begin in early July and last until mid-September and can account for as much as 50%–70% of the annual precipitation in the arid region (Carleton et al. 1990; Douglas et al. 1993; Higgins et al. 1997; Mitchell et al. 2002; Sheppard et al. 2002). The variability of this important moisture source is of particular concern for watershed

Corresponding author address: Katrina Grantz, CU-CADSWES, UCB 421, University of Colorado, Boulder, CO 80309.
E-mail: grantz@colorado.edu

DOI: 10.1175/JCLI4091.1

managers, ranchers, and planners in southwestern North America. Too little summer rainfall has negative agricultural and environmental impacts, while heavy summer thunderstorms present the danger of flash floods. Predicting the variability in the strength, location, and timing of monsoonal precipitation is understandably very important for local communities.

The NAMS is established when the winds shift from a generally westerly direction in winter to southerly flow in summer. These southerly winds bring moist air from the Gulf of California, the eastern Pacific Ocean, and the Gulf of Mexico northward to the land during the summer months (Adams and Comrie 1997). This shift in the winds is brought about by the landmass heating up in summer, thus increasing the land–ocean temperature gradient and bringing the winds from the relatively cooler ocean in over the land. The combination of moist air and warm land surfaces causes convective instability, thus producing frequent summer precipitation events (Adams and Comrie 1997; Barlow et al. 1998). The seasonal shift in the winds depends primarily upon the relative location of the subtropical jet, which typically migrates northward during the summer months. Several studies have shown that a more northward displacement of the subtropical ridge is associated with a wetter monsoon over the southwestern United States. In years when the ridge stays in a more southerly position, the transport of tropical moisture is inhibited (Carleton 1986; Carleton et al. 1990; Adams and Comrie 1997; Comrie and Glenn 1998; Ellis and Hawkins 2001; Hawkins et al. 2002).

Geographically speaking, the NAMS is centered over the Sierra Madre Occidental, a mountain range in northwestern Mexico (Douglas et al. 1993; Barlow et al. 1998); however, it extends into New Mexico, Arizona, southern Colorado, and Utah (e.g., Hawkins et al. 2002; Douglas et al. 1993; Lo and Clark 2002). Several researchers (e.g., Brenner 1974; Hales 1974; Houghton 1979; Tang and Reiter 1984; Reiter and Tang 1984) have defined the NAMS region to be much larger, covering the entire plateau of western North America.

The complex nature of the moisture source and transport mechanism together with varied topography in the region make it extremely difficult to understand the variability of the NAMS. Regionally, the intensity of the NAMS decreases as one moves northward of the Sierra Madre Occidental. Not only is the intensity of the monsoon much weaker in the southwestern United States, but the variability of the monsoon is also much larger in these regions, sometimes larger than the mean summer rainfall itself (Higgins et al. 1998).

The temporal variability of the NAMS ranges from diurnal to seasonal, to interannual, to interdecadal. Diurnal variability is dominated by precipitation peaking in the afternoon and early evening (Dai et al. 1999; Berbery 2001; Trenberth et al. 2003; Anderson and Kanamaru 2005). On an intraseasonal scale, particularly the northern parts of the monsoon region experience wet and dry spells within a monsoon season. This is likely related to a gulf surge phenomenon that brings moisture up the Gulf of California in intermittent bursts (Hales 1972; Brenner 1974). Carleton (1986, 1987) demonstrated that periods of convective activity across the southwestern United States are associated with passing upper-level troughs in the westerlies. Also, as noted earlier, the position of the subtropical ridge significantly affects convective activity (Carleton 1986; Carleton et al. 1990; Adams and Comrie 1997; Comrie and Glenn 1998; Ellis and Hawkins 2001; Hawkins et al. 2002).

Interannual variability is presumed to result from variability in certain synoptic-scale patterns as well as variability in the initial conditions of the landmass and Pacific Ocean SSTs. Carleton et al. (1990) observed that shifts in the subtropical ridge are related to the phase of the PNA (which is related to ENSO), where a positive (negative) PNA pattern in winter is typically followed by a northward (southward) displacement of the subtropical jet and a wet (dry) summer monsoon. Higgins et al. (1999) found that cold (warm) tropical Pacific SST anomalies appear near the date line prior to wet (dry) monsoons and that the anomalies increase in amplitude during the spring. Other studies (Higgins and Shi 2000; Mo and Paegle 2000) have found that anomalously cold SSTs in the northern Pacific and anomalously warm SSTs in the subtropical northern Pacific contribute to a wetter and earlier monsoon season. Castro et al. (2001) observed similar relationships with Pacific SSTs linking a high (low) Pacific decadal oscillation (PDO) phase and El Niño (La Niña) with a southward (northward) displaced monsoon ridge and a late (early) monsoon onset and below (above) average early monsoon rainfall. Mitchell et al. (2002) determined certain threshold SST values for the northern Gulf of California that are associated with the regional onset of the NAMS.

Land surface conditions also play an extensive role in the onset and intensity of the NAMS. Within a monsoon season, increased soil moisture impacts evapotranspiration between storm events, thus enhancing future storm systems and precipitation (Matsui et al. 2003). On an interseasonal scale, several studies have demonstrated an inverse relationship between winter precipitation, particularly snowfall, and subsequent summer precipitation (Gutzler 2000; Higgins and Shi

2000; Lo and Clark 2002; Zhu et al. 2005). This relationship is thought to result from snowfall acting as an energy sink. Greater amounts of snowfall in winter require more energy to melt and evaporate the moisture by summer. Larger snow cover areas also increase the albedo in spring, thus reinforcing the relationship. The resulting delayed and decreased warming of the North American landmass upsets the land–ocean heating contrasts necessary for monsoonal circulation patterns, thus delaying and decreasing the intensity of the NAMS. The relationship between antecedent land conditions and monsoonal precipitation, however, appears to vary spatially and temporally (Lo and Clark 2002; Zhu et al. 2005), and the intensity of the monsoon may depend more on large-scale forcings than local antecedent soil moisture conditions (Zhu et al. 2005). Relationships between monsoonal precipitation and runoff have not been extensively studied, though Gochis et al. (2003) found that runoff in Mexico may depend more on precipitation rates in individual local storms than on monthly total, basin-averaged precipitation.

While several recent studies have illustrated an earlier onset of spring in the western United States (e.g., Dettinger and Cayan 1995; Cayan et al. 2001; Mote 2003; Stewart et al. 2004; Regonda et al. 2005), this has not been studied in relation to the NAMS. Furthermore, there has been relatively little research on the variability of the seasonal cycle of the monsoon, which has important implications for water management and region vulnerability (Ray et al. 2007).

This research sets out to investigate recent trends in the timing and rainfall amount of the NAMS in Arizona and New Mexico and potential large-scale drivers for these trends. Analyses are performed on monthly climate division data and daily COOP station data for the periods 1948–2004 and 1949–99, respectively. Trends are assessed using the Spearman rank correlation analysis and the Kendall–Theil slope estimator, which are robust to outliers and principal component analysis (PCA) is used to extract the dominant spatial patterns. These dominant patterns are then correlated with antecedent land–ocean–atmosphere variables to ascertain driving factors for the NAMS. The paper is organized as follows. Datasets and the analysis methodology are first presented. Variability in the monsoon seasonal cycle and rainfall amounts are described, followed by their links to antecedent land and ocean conditions. A hypothesis for the relationships is also presented.

2. Data and methods

The datasets and the methodology used in this study are described below.

a. Climate division data

Monthly precipitation, temperature, and Palmer drought severity index (PDSI) data from eight climate divisions covering New Mexico and seven divisions for Arizona for the years 1948–2004 were used. The climate divisions and datasets were obtained online (information available at www.cpc.ncep.noaa.gov).

b. NWS COOP data

Daily precipitation data were obtained from the National Weather Service cooperative network (COOP). Most COOP stations have records beginning from the mid-1900s. Stations with continuous daily records from 1948 to 1999 across New Mexico and Arizona were selected—219 stations in total.

c. NCEP–NCAR reanalysis data

Monthly values of large-scale ocean atmospheric variables, for example, sea surface temperature (SST), geopotential heights, precipitable water, winds, etc., from the National Centers for Environmental Prediction–National Center for Atmospheric Research (NCEP–NCAR) reanalysis data (Kalnay et al. 1996) were obtained online (see the Web site http://www.cdc.noaa.gov) for the years 1948–2004.

d. Methodology

To understand the seasonal cycle and "timing" of the monsoon, we first identify the Julian day when the 10th, 25th, 50th, 75th, and 90th percentiles of the monsoonal (July–September) precipitation occurred for each year at all the COOP stations. The Julian day at these five thresholds helps capture the entire monsoon cycle. This provides an objective means for representing the monsoon cycle uniformly across all locations without resorting to subjective definitions for determining the monsoon onset or end.

Nonparametric trend analyses based on the Spearman rank correlation (Helsel and Hirsch 1995) are performed on the 10th, 25th, 50th, 75th, and 90th percentile Julian days at all the stations. The Spearman rank correlation is similar to the standard correlation coefficient (i.e., Pearson's R), except that it does not require that data be normally distributed and it is robust against outliers. To perform the Spearman rank correlation in this study we take one station's time series of Julian days when the 50th percentile of monsoonal precipitation occurred and convert these Julian day values to ranks. These ranks are then plotted against the corresponding year in which the value occurred and a linear regression is fit. We use the robust Kendall–Theil slope

estimator (Helsel and Hirsch 1995) to calculate the magnitude (number of days) and direction (earlier or later) of the timing shift. The Kendall–Theil method is robust to outliers and estimates slope by calculating the median of the slopes between all combinations of two points in the data. This process is repeated for each station and for the other percentiles (10th, 25th, 75th, and 90th) of precipitation. The estimated trends in "timing" are then spatially mapped. Stations exhibiting a trend at the 90% significance level or above are highlighted. The spatial maps of the 90% and 95% significance results were found to be, largely, the same and almost all of them are field significant at the 95% significance level. However, we show the 90% significance figures so as to better illustrate the spatial extent of the trends. Similar analyses are performed on the monsoon monthly and seasonal rainfall amounts as well as the precipitable water. It is recognized that the Spearman rank correlation trend analysis, like other trend analyses, is sensitive to the data at the beginning and the end of the period of record. However, because the Spearman rank correlation trend analysis uses ranks and is thus robust against outliers, the trends are less sensitive to extreme wet periods and dry periods.

The field significance of the spatial patterns of the trends and correlations are determined using the method proposed by Livezey and Chen (1983). For a spatial map to be field significant at the 95% confidence level at least 16 locations (out of 219 COOP stations) and 2 climate divisions (out of 15) should exhibit significant trends and correlations.

To understand the physical mechanisms driving the trends, we analyze the relationship between antecedent (December–May) land–ocean conditions and summer rainfall. First, we perform the Spearman rank correlation analysis to detect trends in antecedent precipitation and soil moisture (we use the PDSI as a proxy for this). We use the PDSI as a surrogate for soil moisture primarily because the quality and quantity of soil moisture data required for this study was unavailable. The PDSI is an integrated measure of rainfall and temperature and is, thus, a good indicator of the soil moisture. Sims et al. (2002) found fairly good correspondence between PDSI and soil moisture in North Carolina, and Guttman et al. (1992) suggested that the PDSI is best suited to semiarid and dry climate regions. Together, these studies suggest that PDSI is an appropriate proxy for soil moisture in the NAMS region.

Next, the leading modes of the timing and rainfall amounts from the summer season are correlated with the antecedent oceanic, atmospheric, and land conditions. The leading modes are obtained by performing principal component analysis (PCA) on the Julian day and monthly rainfall time series. PCA is widely used in climate research. This method decomposes a space–time random field into orthogonal space and time patterns using eigen decomposition and effectively reduces the dimensions of the data (e.g., von Storch and Zwiers 1999). In PCA the patterns are automatically ordered according to the percentage of variance captured; that is, the first space–time pattern, also called the leading mode or first principal component (PC), captures the most variance present in the data, and so on. In this research, for example, the 50th percentile rainfall Julian days of the multivariate data are represented by a 52×219 matrix with the years in rows and the stations in columns. PCA is performed, resulting in 219 PC time series, the first few of which capture most of the variance among the stations. This is repeated for the other Julian day time series (i.e., 10th, 25th, 75th, and 90th percentiles) and the monthly (i.e., July, August, and September) rainfall time series. In all cases the first spatial pattern or eigenvector was found to have similar magnitude and sign across the spatial locations and the first PC was highly correlated with the spatial average time series. We thus use the first PC rather than a straight spatial average to represent the timing and amount across the region. This first PC, as an average spatial index, is correlated with the antecedent oceanic, atmospheric, and land conditions.

Analysis of the rainfall amount is performed using the monthly climate division data since, unlike the COOP data, this dataset extends until the present. The COOP and climate division data, however, are quite consistent, and a comparative analysis found that the results are insensitive to the dataset. For the timing analysis, the daily COOP data are required.

3. Results

The results from the trend analysis of the timing and rainfall amounts are presented first, followed by the relationships to antecedent large-scale climate variables and the physical mechanisms. Based on these results, we put forth a hypothesis for the monsoon variability.

a. Monsoon cycle

Julian day trends at the five threshold levels (10th, 25th, 50th, 75th, and 90th percentile) significant at the 90% level are shown in Fig. 1. It can be seen that there is a significant delay in the entire monsoon cycle (i.e., all five percentiles) over the monsoon region. With well over 21 stations exhibiting a statistically significant trend across the NAMS region, the spatial trend maps are field significant at the 95% confidence level for all

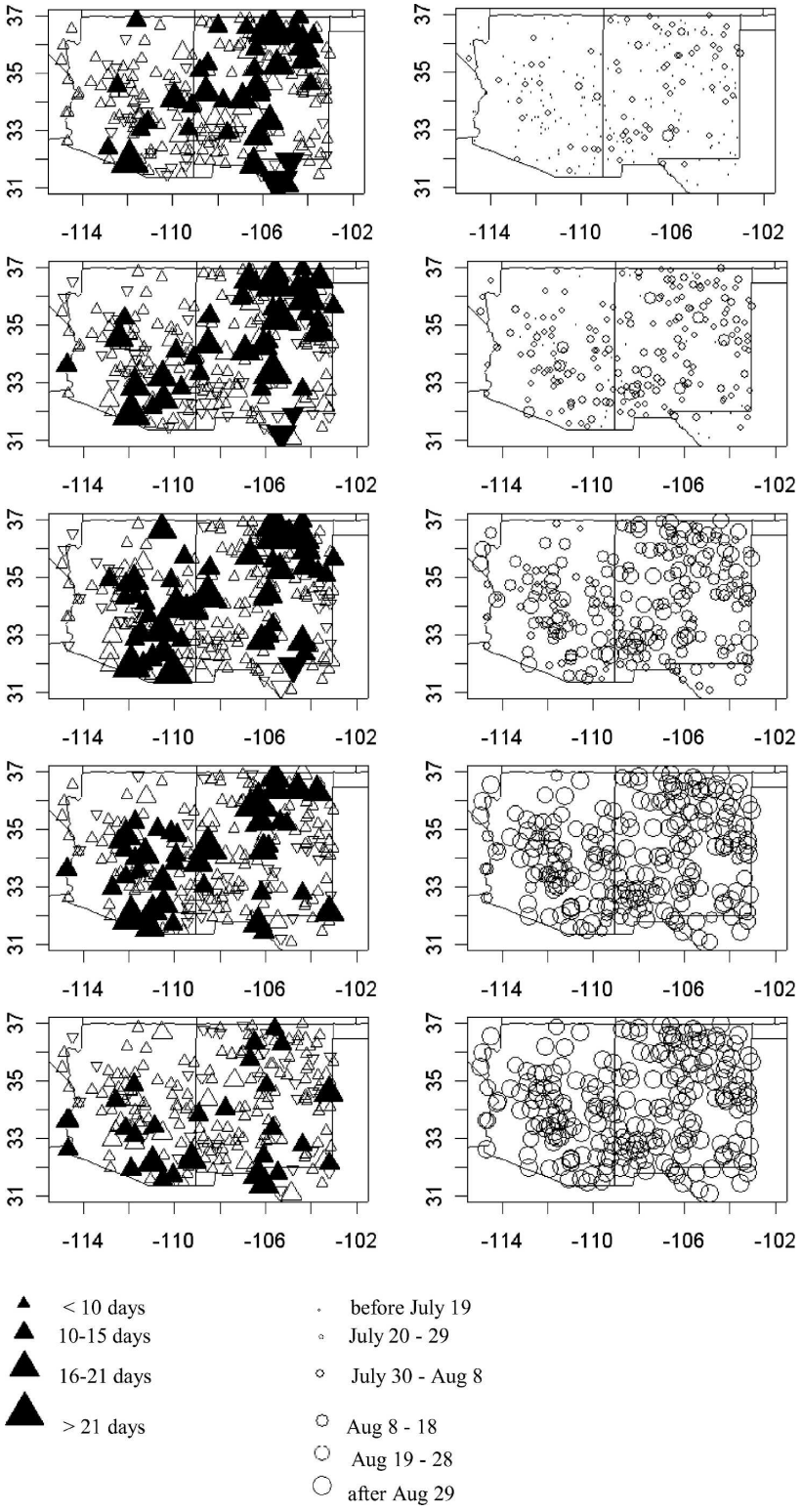

FIG. 1. Trends in Julian day of summer (July–September) seasonal rainfall accumulation at five thresholds (10th, 25th, 50th, 75th, and 90th percentiles; left column, top to bottom, respectively) and the corresponding climatological Julian days (right column, top to bottom, respectively). For the Julian day trends, point-up triangles indicate delay and point-down triangles indicate advancement. Triangle size indicates the magnitude of the trend. Filled triangles indicate 90% significance. For the climatological Julian days, the six circle sizes represent six Julian day windows.

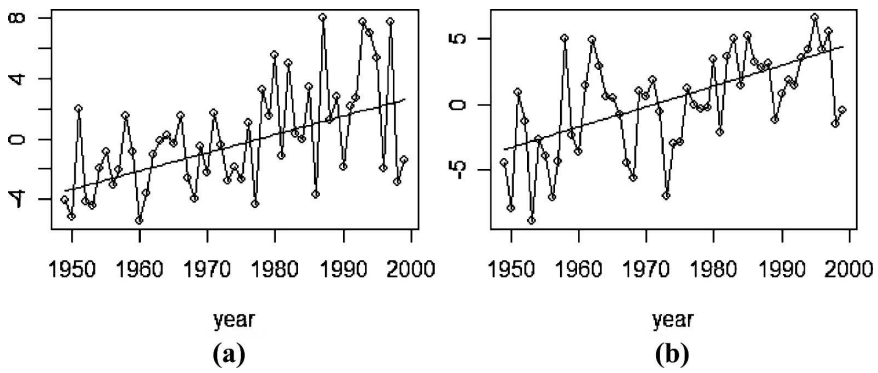

FIG. 2. Time series of PC1 for the Julian day when the (a) 10th and (b) 50th percentiles of the summer (July–September) seasonal rainfall have accumulated. The trend line is the nonparametric Kendall–Theil slope of the data.

threshold percentiles. The shifts are on the order of 10–20 days, depending on the station. To put these shifts in perspective, the median Julian days, that is, the median of all historical data for all stations, for these thresholds are also shown in Fig. 1. Climatologically, the monsoon begins in early July, reaching 10% of the total precipitation by (or on) 19 July; the peak of the monsoon (when 50% of the precipitation has fallen) occurs around 13 August (roughly a week earlier in Arizona than in New Mexico) and the monsoon typically nears its end (when 90% of the total precipitation has fallen) roughly at the end of August and into the beginning of September.

Figure 2 shows the time series of the first PC for the 10th and 50th percentile Julian days. As described in the methodology section, these PCs can be thought of as a spatial average for the region. The trend line shown in the figures is the nonparametric Kendall–Theil slope of the data. As can be seen, the timing PCs exhibit similar trends to those exhibited in the COOP station data presented in Fig. 1.

The timing shift that delays the monsoon cycle would suggest an increase in August and September rainfall and a corresponding decrease in July rainfall. For supporting evidence to the trends seen with the COOP data in Fig. 1 and the timing PCs in Fig. 2, we look at the annual cycle of the rainfall using the monthly climate division data. The annual cycle of the rainfall at four representative climate divisions from the region for the periods 1948–75 and 1976–2004 are shown in Fig. 3. A comparison of the two time periods shows a general decrease in precipitation in July and an increase in August and September from the first half of the period of record to the second. Other climate divisions, particularly those in the lower regions, show similar changes to the annual cycle. These shifts are consistent with the shifts identified in Fig. 1.

b. Monsoon rainfall

Spatial trends in the monthly rainfall amount (July–September) are shown in Fig. 4. It can be seen that precipitation is generally decreasing in July and increasing in August and September, with New Mexico exhibiting a stronger trend. Also, a general increase in total monsoonal precipitation (July–September) is evident largely for New Mexico, which is consistent with the increasing trend in August and September. The spatial trend maps are field significant at the 95% confidence level. The daily COOP station data, which have a shorter period of record, show very similar trend results indicating that the trend is not dependent on the beginning and end of the dataset (figure not shown). To further corroborate this result, we computed the trends in the July–September precipitable water (Fig. 5). The precipitable water shows trends similar to the rainfall results. We note that the trends seen in the timing and rainfall amount should not be used for predictive purposes in and of themselves, but rather as a diagnostic tool to help shed light on the key drivers of monsoon variability.

c. Hypothesis

The key question that emerges from the above analysis is: what is driving the delay in the monsoon cycle? We turn to the "basics" of the monsoon process, that is, the premonsoon land–ocean gradient, for answers. We hypothesize that there is increased antecedent (premonsoon) soil moisture in the southwestern United States that requires longer summer heating and delays the development of the necessary land–ocean temperature gradient, consequently delaying the summer monsoon. It is reasoned that the wetter winter and spring conditions in the southwestern United States are largely driven by winter oceanic–atmospheric condi-

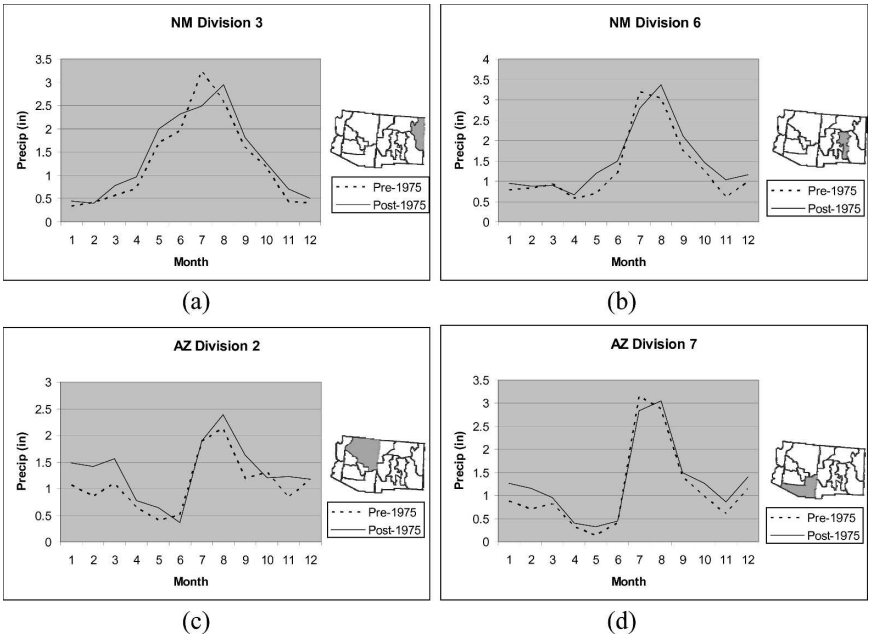

FIG. 3. Annual cycle of precipitation during 1948–75 (dashed line) and 1976–2004 (solid line) at two climate divisions in (a), (b) NM and (c), (d) two climate divisions in AZ.

tions, especially Pacific SSTs, the PDO–ENSO pattern, and the observed increase in ENSO activity in recent decades (Trenberth and Hoar 1996; Rajagopalan et al. 1997). Links to the antecedent land, ocean, and atmosphere conditions offer hope for long-lead forecasts of the summer monsoon. This hypothesis is tested in the following sections. A similar hypothesis was proposed by Zhu et al. (2005) though their hypothesis and analysis focused on the role of the antecedent land and atmosphere conditions (not ocean conditions) and mon-

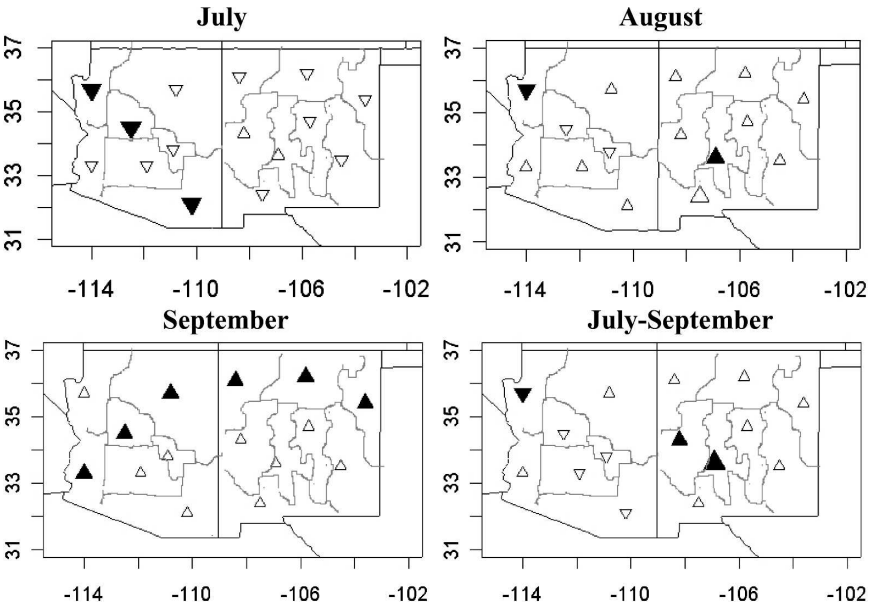

FIG. 4. Trends in summer monthly and seasonal rainfall. Point-up triangles indicate an increasing trend and point-down triangles indicate a decreasing trend. Size indicates the relative magnitude of the trend. For July–September, the triangle sizes correspond to approximately <0.4, 0.4–0.7, and >0.7 in. Filled symbols indicate 90% significance.

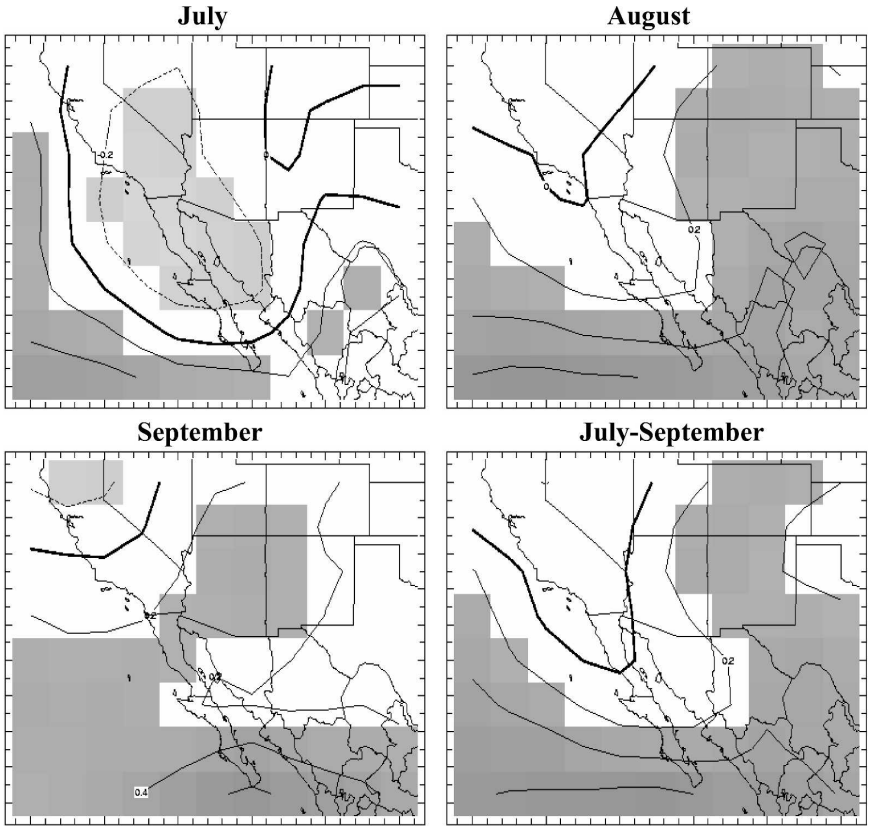

FIG. 5. Trends in monthly and seasonal precipitable water. Shaded regions indicate approximate 90% significance.

soon precipitation in the "monsoon west" region of western New Mexico and eastern Arizona. The results presented below generally corroborate those of Zhu et al. though the analysis and datasets were different.

d. Antecedent land conditions

To determine whether the antecedent land conditions are getting wetter, we examined the trends in the precipitation and PDSI for the December–May season (Fig. 6). A significant increasing trend in the winter–spring precipitation and PDSI over the desert Southwest can be seen. Also, a corresponding decreasing trend over the Pacific Northwest is apparent. These trends are also field significant at the 95% confidence level. Increased precipitation in the southwest and decreased precipitation in the northwest is typical of ENSO teleconnections in the western United States, as identified by several researchers (Ropelewski and Halpert 1986; Redmond and Koch 1991; Cayan and Webb 1992; Cayan et al. 1999).

To further demonstrate the strength of the link between antecedent land conditions and the timing of the monsoon, we correlate the leading mode of the monsoon timing with the premonsoon land conditions. The first PC explains 28% of the total variance and the first eigenvector has similar magnitude and sign across all stations; hence, the first PC can be regarded as the regional monsoon "timing index." Figures 7a and 7b shows the correlations between the first PC for the monsoon peak, that is, the Julian day when the 50th percentile of the total seasonal rainfall has occurred, and the winter–spring (December–May) precipitation and PDSI. Significant positive correlations exist between the regional monsoon timing index and antecedent precipitation and PDSI over the monsoon region. These positive correlations indicate that an increase in the monsoon peak's Julian day (i.e., a late shift in the monsoon) occurs with increased rainfall and soil moisture during the preceding winter/spring, thus supporting the proposed hypothesis. When the timing of the onset of the monsoon is considered, this correlation pattern becomes even stronger. Figures 7c and 7d present the correlations between the first PC of the onset (i.e., the Julian day when the 10th percentile of the seasonal rainfall has occurred) and the antecedent conditions. The 10th percentile PC captures 31% of the

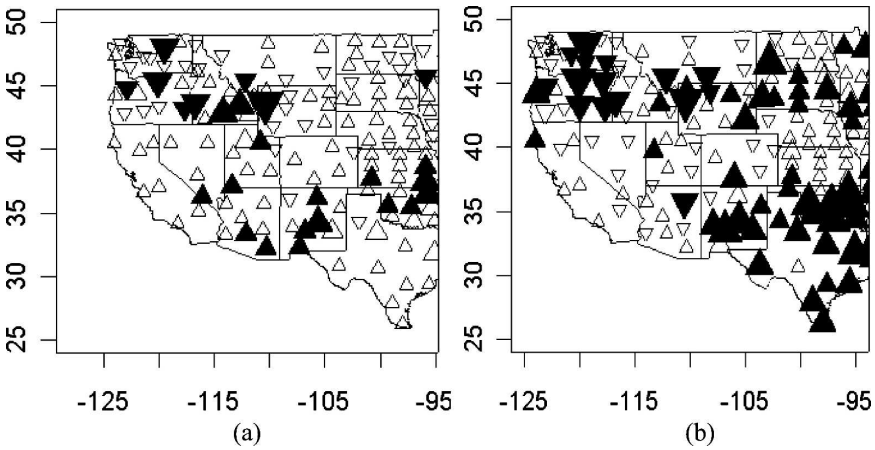

FIG. 6. Trends in antecedent winter–spring (December–May) land conditions: (a) precipitation and (b) PDSI. Point-up triangles indicate an increasing trend, and point-down triangles, a decreasing trend. Symbol size indicates the relative magnitude of the trend and filled symbols indicate 90% significance.

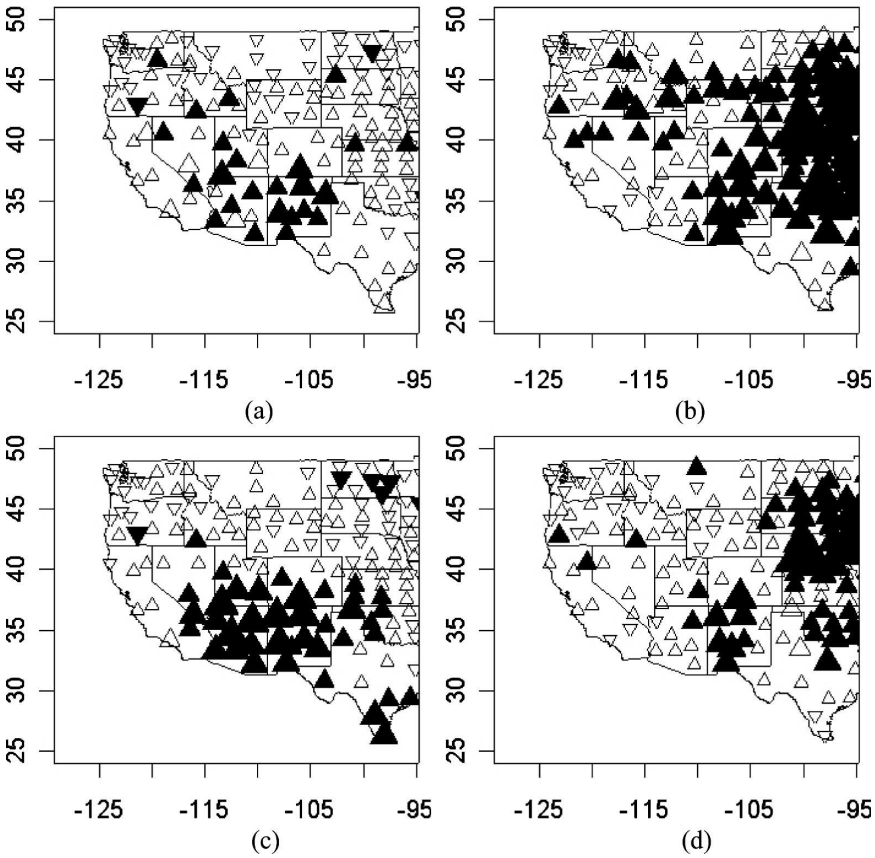

FIG. 7. Correlation map of the (a), (b) 50th and (c), (d) 10th percentiles of the timing PC with (a), (c) antecedent winter–spring precipitation and (b), (d) PDSI. Point-up triangles indicate a positive correlation, and point-down indicate a negative correlation. Symbol size indicates the relative magnitude of the correlation and filled symbols indicate 90% significance.

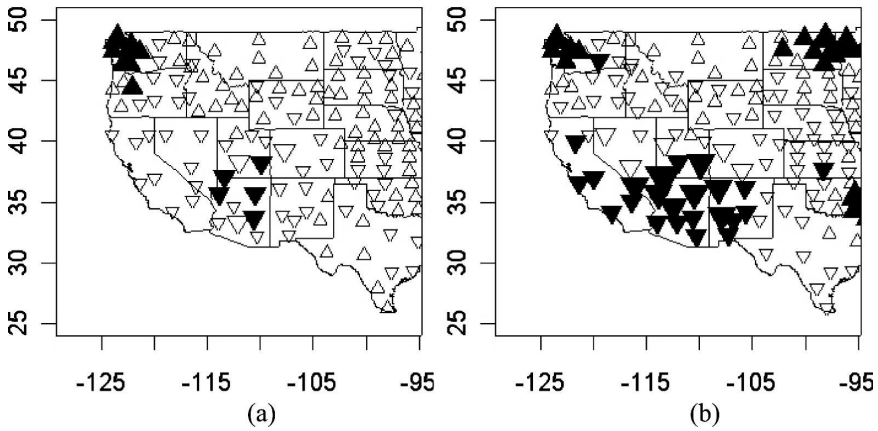

FIG. 8. Correlation map of the rainfall amount's first PC for (a) July–September and (b) July with antecedent winter–spring precipitation. Point-up triangles indicate a positive correlation, and point-down triangles indicate a negative correlation. Symbol size indicates the relative magnitude of the correlation and filled symbols indicate 90% significance.

total variance and can be thought of as the leading mode of the monsoon onset. It is noted that the relatively low values of 28% and 31% of the total variance accounted for by the first PC can be explained by the noise in the daily data. The leading PC in all of the cases, however, provides a robust measure of the spatial average.

Correlations between the leading mode of the summer (July–September) monsoon rainfall amount and antecedent precipitation (Fig. 8a) show a negative correlation pattern over the monsoon region and a positive trend over the northwestern United States. The results are similar for the antecedent PDSI (figures not shown). Interestingly, the correlation pattern for the leading mode of the July rainfall amount (Fig. 8b) is even stronger, indicating that the onset of the monsoon is most affected by antecedent conditions. These results are consistent with the timing results presented above: as premonsoon land moisture increases, the monsoon is delayed, thus decreasing monsoonal precipitation in July. The negative relationship between winter–spring precipitation and summertime precipitation over the southwestern United States has also been noted in previous studies (e.g., Gutzler 2000; Lo and Clark 2002). Similar results were obtained when the PCA was performed separately for Arizona precipitation and New Mexico precipitation and each of these leading PCs was correlated with antecedent land conditions. In general, correlations with Arizona tended to be slightly stronger. Table 1 shows the percent of total variance captured by the leading PCs.

These results indicate that the preceding winter–spring land conditions (i.e., precipitation, soil moisture) tend to most strongly affect the timing of the monsoon initiation and the early monsoon rainfall amount (i.e., July rainfall). That is, a wetter winter–spring tends to delay the monsoon cycle and decrease monsoon rainfall in July, and vice versa.

e. Antecedent ocean conditions

It is generally accepted that the enhanced wet (dry) conditions over the southwestern (northwestern) United States in winter and spring seasons are largely due to warm ENSO conditions (Ropelewski and Halpert 1986; Redmond and Koch 1991; Cayan and Webb 1992; Cayan et al. 1999). Consequently, winter and spring ocean conditions should also be related to the following monsoon. To investigate this explicitly, we relate the monsoon attributes (timing and rainfall amount) to antecedent ocean conditions.

Correlations between the winter–spring (December–May) SSTs and the leading mode of the following mon-

TABLE 1. Percent of total variance captured by each leading PC of monsoonal precipitation in varying months and regions.

State	Month	Variance (%)
AZ, NM	Jul	45
AZ, NM	Aug	53
AZ, NM	Sep	58
AZ, NM	Jul–Sep	43
AZ	Jul	80
AZ	Aug	78
AZ	Sep	75
AZ	Jul–Sep	77
NM	Jul	61
NM	Aug	64
NM	Sep	71
NM	Jul–Sep	63

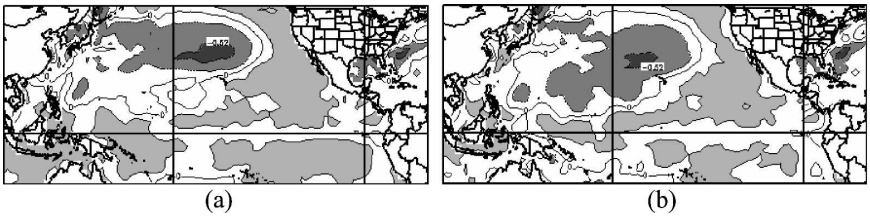

FIG. 9. Correlations between the winter–spring (December–May) SSTs and the first PC of the Julian day of the (a) 50th and (b) 10th percentiles. Correlations above 0.25 and below –0.25 are 90% significant. Shaded regions are statistically significant at the 90% confidence level. (Images provided by the NOAA–CIRES Climate Diagnostics Center, Boulder, CO, from their Web site: http://www.cdc.noaa.gov/.)

soon's peak Julian day exhibit strong negative values (between −0.5 and −0.6) in the northern Pacific Ocean (Fig. 9a) around 30°N, just east of the date line. Weaker positive correlations are seen to the southeast of this region (around 10°N) and in the tropical Pacific. This pattern is larger and stronger with the leading mode of the early monsoon Julian day (Fig. 9b). Shaded regions are statistically significant at the 90% confidence level based on the normal test for the correlation coefficient (Helsel and Hirsch 1995). These correlations indicate that a dipole pattern of below average SSTs in the North Pacific and above average SSTs to the southeast and in the tropical Pacific in winter–spring tend to increase (i.e., delay) the monsoon timing. We hypothesize that this occurs via an increased winter–spring precipitation over the monsoon region resulting in a weaker land–ocean gradient, which delays the monsoon cycle (Figs. 5 and 6). Though ENSO activity has been shown to increase winter and spring precipitation in the southwest United States, the SST correlation pattern with the monsoon timing does not show an explicit ENSO pattern.

We correlated the leading mode of the monthly and summer seasonal monsoon rainfall amounts with the antecedent ocean conditions (Fig. 10). The SST patterns for the July rainfall (Fig. 10a) show positive correlations (between +0.4 and +0.5) in the northern Pacific region (same as in Fig. 9) and negative correlations (between −0.3 and −0.4) to the southeast of this region extending down to the Tropics. That is, warmer northern Pacific SSTs and cooler tropical Pacific SSTs during winter–spring are related to increased monsoon rainfall during July. We hypothesize that these SST conditions result in decreased winter–spring precipitation over the southwest United States (e.g., Ropelewski and Halpert 1986), increasing the land–ocean temperature gradient and the resulting monsoonal precipitation in July. The correlation pattern reverses and is much weaker (Figs. 9b–d) for the August, September, and total seasonal precipitation amounts. In August, the correlations are between +0.3 and +0.4 in the northern Pacific and between −0.2 and −0.3 to the south and east. By September the correlations are not statistically significant. This indicates that the antecedent winter–spring ocean con-

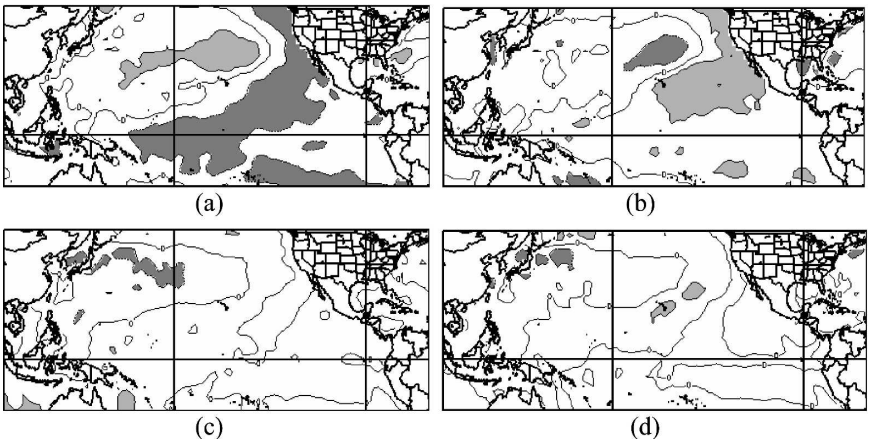

FIG. 10. Same as in Fig. 9 except for correlations between the winter–spring (December–May) SSTs and the first PC of the (a) July, (b) August, (c) September, and (d) July–September monsoon rainfall.

ditions have a stronger impact on the early monsoon (July) rainfall. This is consistent with the results obtained for the antecedent land conditions described in the previous section.

This leaves us to question what large-scale features, if any, affect the late monsoon (August–September) rainfall. To explore this, we correlated the leading modes of August and September rainfall with the near-term and concurrent ocean conditions. The leading mode of rainfall in these months is related to SSTs near the California coast and Gulf of California, where correlations are above +0.4 and are stronger for August than for September (figures not shown). These results generally corroborate those of Kim et al. (2005) who showed through modeling that increases in SSTs around the Gulf of California are linked with increased monsoonal precipitation after the onset of the monsoon.

4. Summary and conclusions

A systematic analysis of the spatiotemporal attributes of NAMS in Arizona and New Mexico was performed in this study. Trends in the Julian day of summer rainfall indicate a significant delay (approximately 10–20 days) in the entire cycle of the summer monsoon in Arizona and New Mexico. This delay in the monsoon cycle is manifested with a decrease in rainfall during the early monsoon (July) and corresponding increase during the later period (August–September). The antecedent (winter/spring) rainfall and PDSI show an increasing trend over the southwestern U.S. monsoon region and a decreasing trend over the northwestern United States; this is consistent with the well-known ENSO teleconnections in the western United States. Combining these observations we proposed the following hypothesis: increased antecedent (premonsoon) soil moisture in the monsoon region will take longer summer heating to set up the land–ocean gradient and consequently delay the monsoon cycle. The wetter antecedent conditions in the southwestern United States are largely driven by winter oceanic–atmospheric conditions, especially ENSO. Correlations between antecedent SSTs and the leading modes of the monsoon timing and rainfall amount show that the monsoon (particularly the early monsoon) is related to winter–spring SSTs in the tropical–extratropical Pacific; however, no explicit ENSO pattern emerged in this study. These antecedent links to the land and ocean offer hopes for long-lead forecasts of the summer monsoon. The late season monsoon precipitation appears to be more related to SSTs near the Gulf of California. Further analysis using climate models is needed to more rigorously test the proposed hypothesis. Analysis of the space–time variability of streamflow in the monsoon region is under way to investigate the consistency of the proposed hypothesis and to help in developing long-lead streamflow forecast tools.

Acknowledgments. We thankfully acknowledge the funding of this research by the NOAA Office of Global Program's GAPP project (NA03OAR4310063). Useful discussions with David Gochis and Bruce Anderson are also greatly appreciated. We also thank the three anonymous reviewers for their comments and suggestions for improving the manuscript.

REFERENCES

Adams, D. K., and A. C. Comrie, 1997: The North American monsoon. *Bull. Amer. Meteor. Soc.,* **78,** 2197–2213.

Anderson, B., and H. Kanamaru, 2005: The diurnal cycle of the summertime hydrologic atmospheric cycle over the southwestern United States. *J. Hydrometeor.,* **6,** 219–228.

Barlow, M., S. Nigam, and E. H. Berbery, 1998: Evolution of the North American monsoon system. *J. Climate,* **11,** 2238–2257.

Berbery, E. H., 2001: Mesoscale moisture analysis of the North American monsoon. *J. Climate,* **14,** 121–137.

Brenner, I. S., 1974: A surge of maritime tropical air—Gulf of California to the southwestern United States. *Mon. Wea. Rev.,* **102,** 375–389.

Carleton, A. M., 1986: Synoptic–dynamic character of "bursts" and "breaks" in the southwest U.S. summer precipitation singularity. *J. Climate,* **6,** 605–623.

——, 1987: Summer circulation climate of the American southwest: 1945–1984. *Ann. Assoc. Amer. Geogr.,* **77,** 619–634.

——, D. A. Carpenter, and P. J. Weser, 1990: Mechanisms of interannual variability of southwest United States summer precipitation maximum. *J. Climate,* **3,** 999–1015.

Castro, C. L., T. B. McKee, and R. A. Pilke, 2001: The relationship of the North American monsoon to tropical and North Pacific surface temperatures as revealed by observational analysis. *J. Climate,* **14,** 4449–4473.

Cayan, D. R., and R. H. Webb, 1992: El Niño/Southern Oscillation and streamflow in the western United States. *El Niño: Historical and Paleoclimate Aspects of the Southern Oscillation,* H. F. Diaz and V. Markgraf, Eds., Cambridge University Press, 29–86.

——, K. T. Redmond, and L. G. Riddle, 1999: ENSO and hydrologic extremes in the western United States. *J. Climate,* **12,** 2881–2893.

——, S. A. Kammerdiener, M. D. Dettinger, J. M. Caprio, and D. H. Peterson, 2001: Changes in the onset of spring in the western United States. *Bull. Amer. Meteor. Soc.,* **82,** 399–415.

Comrie, A. C., and E. C. Glenn, 1998: Principal components-based regionalization of precipitation regimes across the southwest United States and northern Mexico, with an application to monsoon precipitation variability. *Climate Res.,* **10,** 201–215.

Dai, A., F. Giorgi, and K. E. Trenberth, 1999: Observed and model-simulated diurnal cycles of precipitation over the contiguous United States. *J. Geophys. Res.,* **104,** 6377–6402.

Dettinger, M. D., and D. R. Cayan, 1995: Large-scale atmospheric forcing of recent trends toward early snowmelt runoff in California. *J. Climate,* **8,** 606–623.

Douglas, M. W., R. A. Maddox, K. Howard, and S. Reyes, 1993: The Mexican monsoon. *J. Climate,* **6,** 1665–1677.

Ellis, A. W., and T. W. Hawkins, 2001: An apparent atmospheric teleconnection between snow cover and the North American monsoon. *Geophys. Res. Lett.,* **28,** 2653–2656.

Gochis, D. J., J. W. Shuttleworth, and Z. Yang, 2003: Hydrometeorological response of the modeled North American monsoon to convective parameterization. *J. Hydrometeor.,* **4,** 235–250.

Guttman, N. B., J. R. Wallis, and J. R. M. Hosking, 1992: Spatial comparability of the Palmer drought severity index. *Water Resour. Bull.,* **28,** 1111–1119.

Gutzler, D. S., 2000: Covariability of spring snowpack and summer rainfall across the southwest United States. *J. Climate,* **13,** 4018–4027.

Hales, J. E., 1972: Surges of maritime tropical air northward over the Gulf of California. *Mon. Wea. Rev.,* **100,** 298–306.

——, 1974: The southwestern United States summer monsoon source—Gulf of Mexico or Pacific Ocean. *J. Appl. Meteor.,* **13,** 331–342.

Hawkins, T. W., A. W. Ellis, J. A. Skindlov, and D. Reigle, 2002: Intraannual analysis of the North American snow cover–monsoon teleconnection: Seasonal forecasting utility. *J. Climate,* **15,** 1743–1753.

Helsel, D. R., and R. M. Hirsch, 1995: *Statistical Methods in Water Resources.* Elsevier Science, 522 pp.

Higgins, R. W., and W. Shi, 2000: Dominant factors responsible for interannual variability of the summer monsoon in the southwestern United States. *J. Climate,* **13,** 759–776.

——, Y. Yao, and X. L. Wang, 1997: Influence of the North American monsoon system on the U.S. summer precipitation regime. *J. Climate,* **10,** 2600–2622.

——, K. C. Mo, and Y. Yao, 1998: Interannual variability of the U.S. summer precipitation regime with emphasis on the southwestern monsoon. *J. Climate,* **11,** 2582–2606.

——, Y. Chen, and A. V. Douglas, 1999: Interannual variability of the North American warm season precipitation regime. *J. Climate,* **12,** 653–680.

Houghton, J. G., 1979: A model for orographic precipitation in the north-central Great Basin. *Mon. Wea. Rev.,* **107,** 1462–1475.

Kalnay, E., and Coauthors, 1996: The NCEP/NCAR 40-Year Reanalysis Project. *Bull. Amer. Meteor. Soc.,* **77,** 437–471.

Kim, J., J. Kim, J. D. Farrara, and J. O. Roads, 2005: The effects of the Gulf of California SSTs on warm-season rainfall in the southwestern United States and northwestern Mexico: A regional model study. *J. Climate,* **18,** 4970–4992.

Livezey, R. E., and W. Y. Chen, 1983: Statistical field significance and its determination by Monte Carlo techniques. *Mon. Wea. Rev.,* **111,** 46–59.

Lo, F., and M. P. Clark, 2002: Relationships between spring snow mass and summer precipitation in the southwestern United States associated with the North American monsoon system. *J. Climate,* **15,** 1378–1385.

Matsui, T., V. Lakshmi, and E. Small, 2003: Links between snow cover, surface skin temperature, and rainfall variability in the North American monsoon system. *J. Climate,* **16,** 1821–1829.

Mitchell, D. L., D. Ivanova, R. Rabin, T. J. Brown, and K. Redmond, 2002: Gulf of California sea surface temperature and the North American monsoon: Mechanistic implication from observation. *J. Climate,* **15,** 2261–2281.

Mo, K. C., and J. N. Paegle, 2000: Influence of sea surface temperature anomalies on the precipitation regimes over the southwest United States. *J. Climate,* **13,** 3588–3598.

Mote, P. W., 2003: Trends in snow water equivalent in the Pacific Northwest and their climatic causes. *Geophys. Res. Lett.,* **30,** 1601, doi:1.1029/2003GL017258.

Rajagopalan, B., U. Lall, and M. A. Cane, 1997: Anomalous ENSO occurrences: An alternate view. *J. Climate,* **10,** 2351–2357.

Ray, A. J., G. M. Garfin, M. Wilder, M. Vásquez-Léon, M. Lenart, and A. C. Comrie, 2007: Applications of monsoon research: Opportunities to inform decision making and reduce regional vulnerability. *J. Climate,* **20,** 1608–1627.

Redmond, K. T., and R. W. Koch, 1991: Surface climate and streamflow variability in the western United States and their relationship to large-scale circulation indices. *Water Resour. Res.,* **27,** 2381–2399.

Regonda, S., B. Rajagopalan, M. Clark, and J. Pitlick, 2005: Seasonal cycle shifts in hydroclimatology over the western United States. *J. Climate,* **18,** 372–384.

Reiter, E. R., and M. Tang, 1984: Plateau effects on diurnal circulation patterns. *Mon. Wea. Rev.,* **112,** 638–651.

Ropelewski, C. F., and M. S. Halpert, 1986: North American precipitation and temperature patterns associated with El Niño/Southern Oscillation (ENSO). *Mon. Wea. Rev.,* **114,** 2352–2362.

Sheppard, P. R., A. C. Comrie, G. D. Packin, K. Angersbach, and M. K. Hughes, 2002: The climate of the U.S. southwest. *Climate Res.,* **21,** 219–238.

Sims, A. P., S. N. Devdutta, and S. Raman, 2002: Adopting drought indices for estimating soil moisture: A North Carolina case study. *Geophys. Res. Lett.,* **29,** 1183, doi:10.1029/2001GL013343.

Stewart, I. T., D. R. Cayan, and M. D. Dettinger, 2004: Changes in snowmelt runoff timing in western North America under a "business as usual" climate change scenario. *Climatic Change,* **62,** 217–232.

Tang, M., and E. R. Reiter, 1984: Plateau monsoons of the Northern Hemisphere: A comparison between North America and Tibet. *Mon. Wea. Rev.,* **112,** 617–637.

Trenberth, K. E., and T. J. Hoar, 1996: The 1990–1995 El Niño–Southern Oscillation event: Longest on record. *Geophys. Res. Lett.,* **23,** 57–60.

——, A. G. Da, R. M. Rasmussen, and D. P. Parsons, 2003: The changing character of precipitation. *Bull. Amer. Meteor. Soc.,* **84,** 1205–1217.

von Storch, H., and F. W. Zwiers, 1999: *Statistical Analysis in Climate Research.* Cambridge University Press, 484 pp.

Zhu, C., D. Lettenmaier, and T. Cavazos, 2005: Role of antecedent land surface condtions on North American monsoon rainfall variability. *J. Climate,* **18,** 3104–3121.